Supplemental Information

Current Biology, Volume *21*

ATP Hydrolysis Is Required for Relocating Cohesin from Sites Occupied by Its Scc2/4 Loading Complex

Bin Hu, Takehiko Itoh, Ajay Mishra, Yuki Katoh, Kok-Lung Chan, William Upcher, Camilla Godlee, Maurici B. Roig, Katsuhiko Shirahige, and Kim Nasmyth

Figure S1.

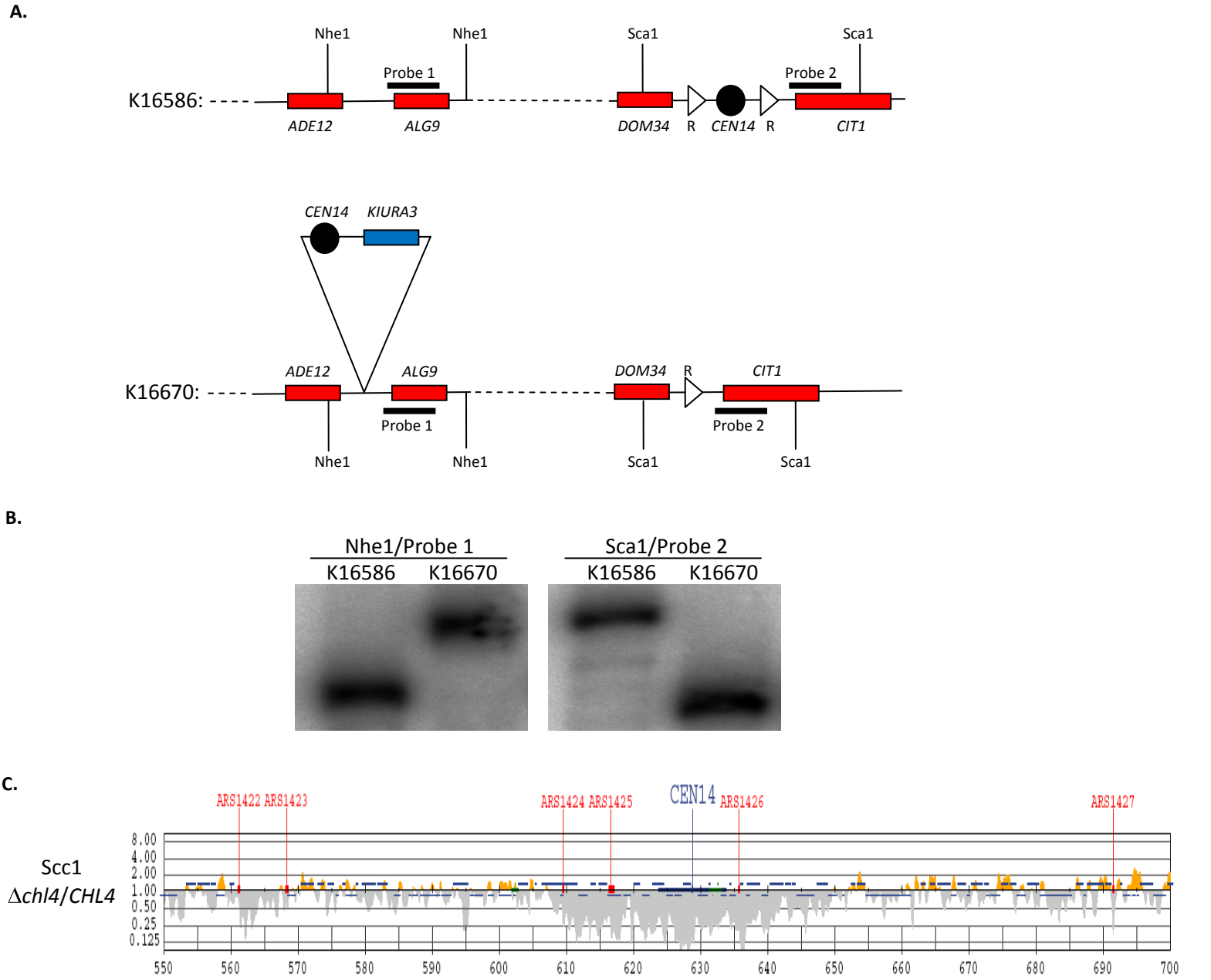

Figure S1. Centromeres promoter cohesin's accumulation at core-cen and peri-cen, related to Figure 1

(A) Strategy for translocalization of cen14 into the site between ADE12 and ALG9 .

(B) Genome DNA extracted from yeast strains K16586 and K16670 were digested by Nhe1 or Sca1 and applied to Southern blot with indicated probe.

(C) Chl4 promotes recruitment of cohesin to centromeres. The ratios of Scc1 ChIP-SEQ signals between Chl4 WT and deletion were mapped to Chromosome XIV.

Figure S2.

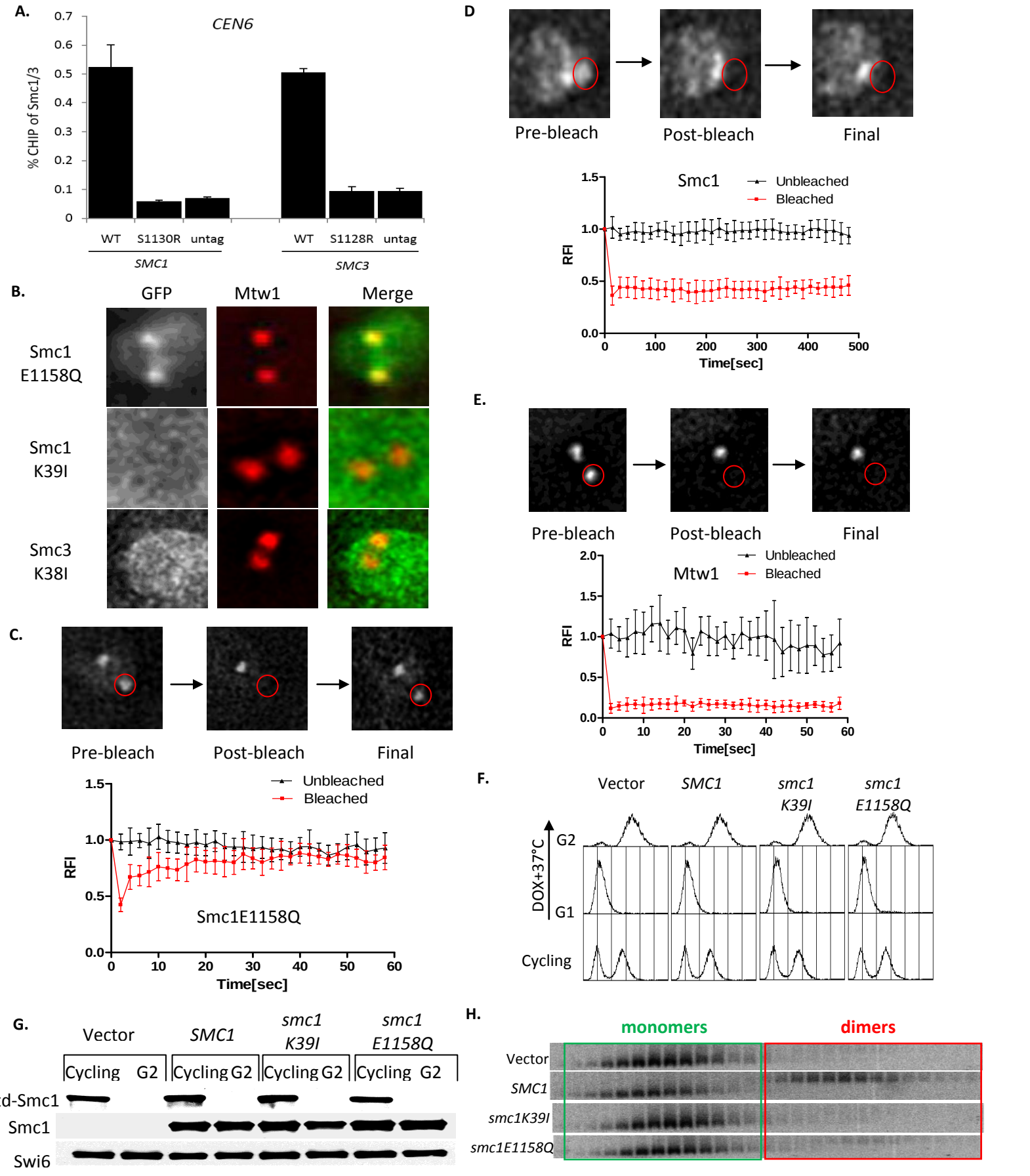
A.
CEN6
% CHIP of Smc1/3
WT
S1130R
untag
WT
S1128R
untag
SMC1
SMC3
B.
GFP
Mtw1
Merge
Smc1 E1158Q
Smc1 K39I
Smc3 K38I
C.
Pre-bleach
Post-bleach
Final
Unbleached
Bleached
RFI
Smc1E1158Q
Time[sec]
D
Pre-bleach
Post-bleach
Final
Smc1
Unbleached
Bleached
RFI
Time[sec]
E.
Pre-bleach
Post-bleach
Final
Mtw1
Unbleached
Bleached
RFI
Time[sec]
F.
Vector
SMC1
smc1 K39I
smc1 E1158Q
DOX+37°C
G2
G1
Cycling
G.
Vector
SMC1
smc1 K39I
smc1 E1158Q
Cycling
G2
td-Smc1
Smc1
Swi6
H.
monomers
dimers
Vector
SMC1
smc1K39I
smc1E1158Q

Figure S2. ATP-dependent engagement of nucleotide binding domains of Smc1/3 is required for cohesin's association at centromere, related to Figure 2

(A) Mutations in signal motif of Smc1/3 prevent chromatin association. ChIP-qPCR was performed for the quantitative measurement of chromatin association of Myc9 or HA3 tagged Smc1/3 WT and corresponding signal motif mutants (K699, K11850, K11852, K11854 and K11574) at Cen6. Error bars represent std. dev.; n=3.

(B) Localization of Smc1E1158Q, Smc1K391 and Smc3K38I. Live cell imaging showed GFP tagged Smc1E1158Q (K16445) colocalized with Mtw1, whereas Smc1K391-GFP was excluded from nuclear and Smc3K38I-GFP showed a diffused nuclear signal.

(C) Association of Smc1E1158Q at centromere was dynamic. FRAP assay revealed Smc3E1155Q-GFP rapidly recovered with $t_{1/2}$ = 3.8 sec after photobleach; n=6; *error bars* represent std dev.

(D) and (E) Stability of association of Smc1 and Mtw1 with chromosomes in centomeric regions. FRAP assay revealed Smc1 (D) and Mtw1 (E) stably associated with centromeres or peri-cen (K16444).

(F-H) Hydrolysis defective cohesin cannot establish cohesion. Exponential phase cells of strains (K16335-8) were arrested at G1 with α-factor at 25°C. Endogenous td-Smc1 was degraded by shifting cultures to the degron-mediated proteolysis conditions (YEP gal, 20 μg/ml doxycycline, 37°C) for 1 hr (F). Subsequently the cells were released from G1 arrest to YEP gal media containing 20 μg/ml doxycycline and 10 μg/ml nocodazole. The cells were lysed and extracts were fractionated by sucrose gradient centrifugation followed by gel electrophoresis. FACS analysis showed that all strains completed DNA replication in the above conditions (F) and degradation of endogenous degron tagged Smc1 were measured by western blot (G). Minichromosome DNA was detected by Southern blotting. Monomers and dimers are marked inside the green and red boxes respectively (H).

Figure S3.

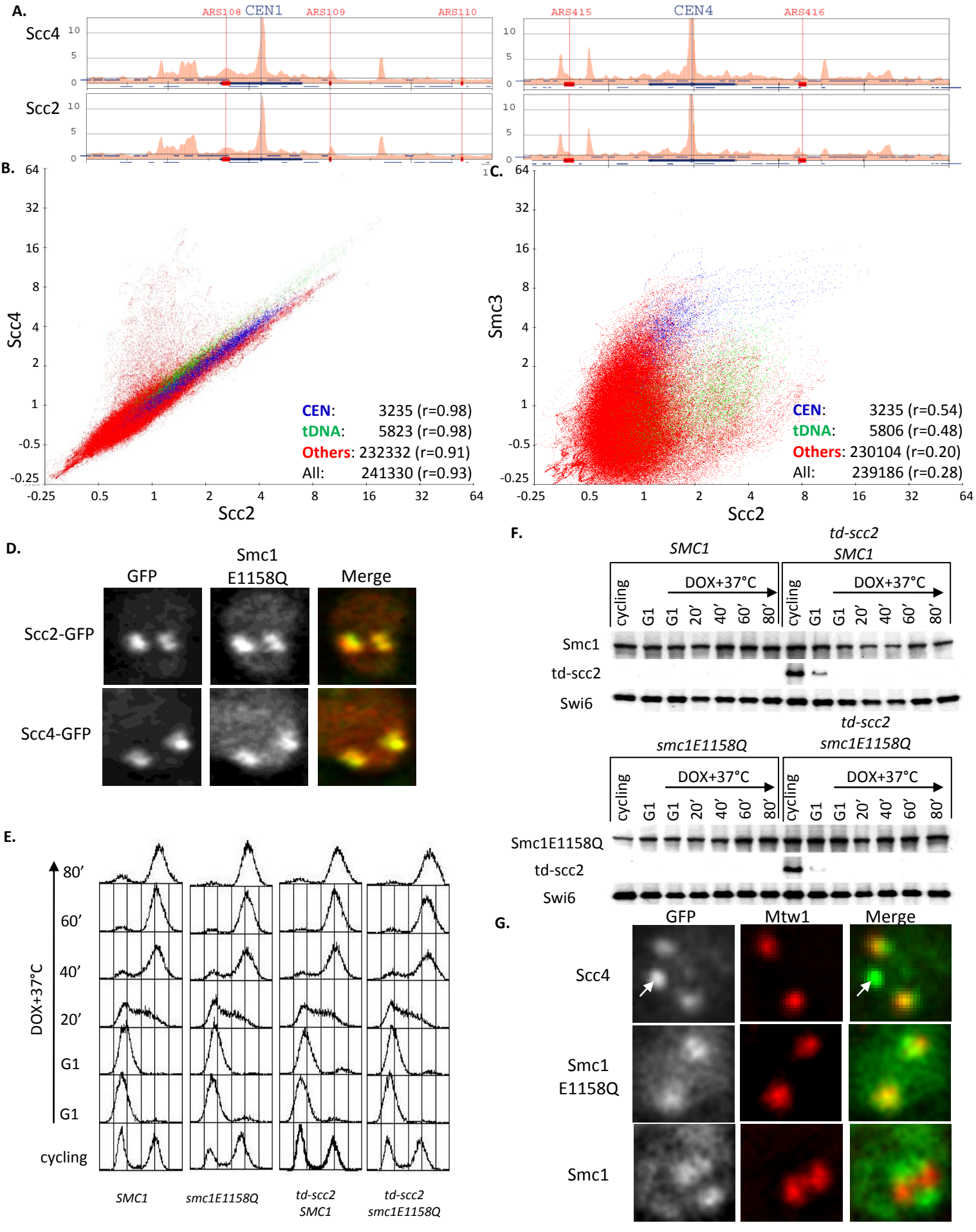
A.
ARS108
CEN1
ARS109
ARS110
ARS415
CEN4
ARS416
Scc4
Scc2
B.
Scc4
Scc2
CEN: 3235 (r=0.98)
tDNA: 5823 (r=0.98)
Others: 232332 (r=0.91)
All: 241330 (r=0.93)
C.
Smc3
Scc2
CEN: 3235 (r=0.54)
tDNA: 5806 (r=0.48)
Others: 230104 (r=0.20)
All: 239186 (r=0.28)
D.
GFP
Smc1 E1158Q
Merge
Scc2-GFP
Scc4-GFP
E.
DOX+37°C
80'
60'
40'
20'
G1
G1
cycling
SMC1
smc1E1158Q
td-scc2 SMC1
td-scc2 smc1E1158Q
F.
SMC1
td-scc2 SMC1
cycling
G1
G1
20'
40'
60'
80'
DOX+37°C
Smc1
td-scc2
Swi6
smc1E1158Q
td-scc2 smc1E1158Q
Smc1E1158Q
G.
GFP
Mtw1
Merge
Scc4
Smc1 E1158Q
Smc1

Figure S3. Hydrolysis defective cohesin co-localized with and depends on Scc2/4, related to Figure 3

(A) Genome-wide distribution of Scc2 and Scc4. Crude extracts prepared from exponentially grown yeast cells (K17458 and K17459) were used for ChIP-SEQ analyses. The distributions of Scc2 and Scc4 at a selected region of chromosome I (top panel) and IV (bottom panel) were shown.

(B) Correlation of Scc2 with Scc2 performed as described in Figure 2C.

(C) Correlation of Smc3 with Scc2 performed as described in Figure 2C.

(D) Hydrolysis defective cohesin co-localized with Scc2/4. Live cell imaging showed RFP tagged Smc1E1158Q (K17026 and K17027) colocalized with Scc2-GFP or Scc4-GFP.

(E) and (F) FACS analysis and Western bolt for Figure 3E.

(G) Artificial tethering of Scc2-tTR to a cluster of Tet operators recruits Scc4 but not hydrolysis defective cohesin. Scc4-GFP, or Smc1E1158Q-GFP was expressed in strains containing 224x Tet operators inserted 38 Kb from CEN5 whose endogenous Scc2 was fused with tTR (K16535 and K16537). Scc4-GFP forms an extra focus indicated by an arrow at URA3 as well as a pair of centromeric foci co-localizing with Mtw1-RFP. In contrast, Smc1E1158Q-GFP only co-localizes with Mtw1-RFP clusters.

Figure S4.

A.

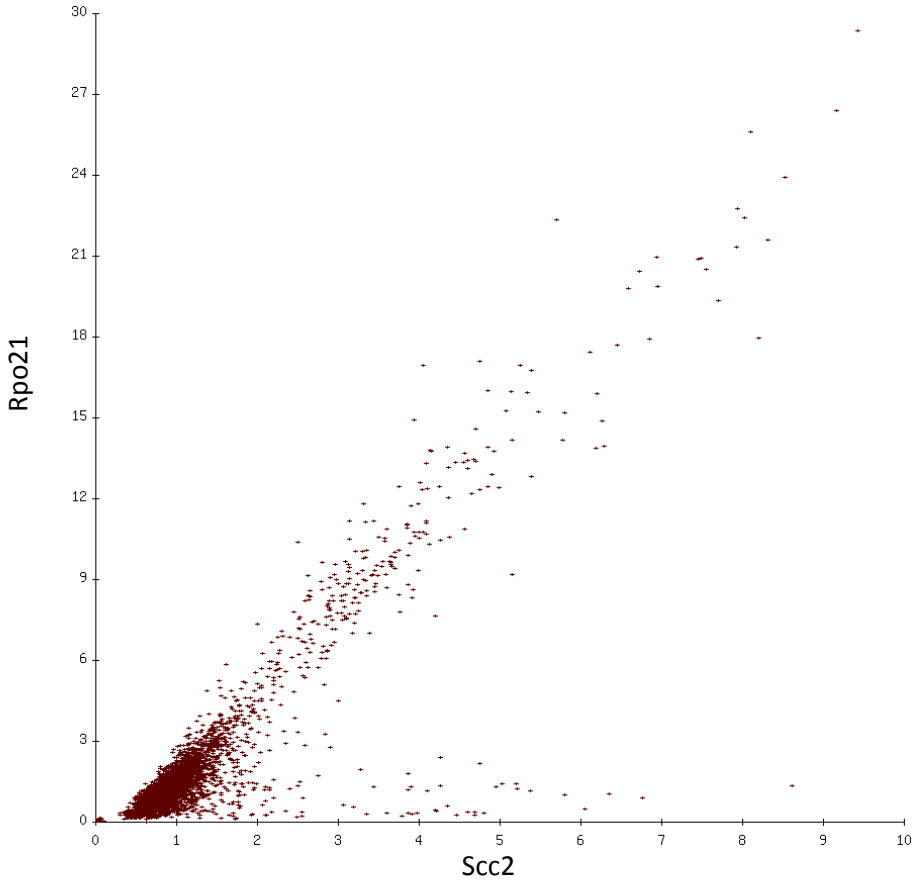

B.

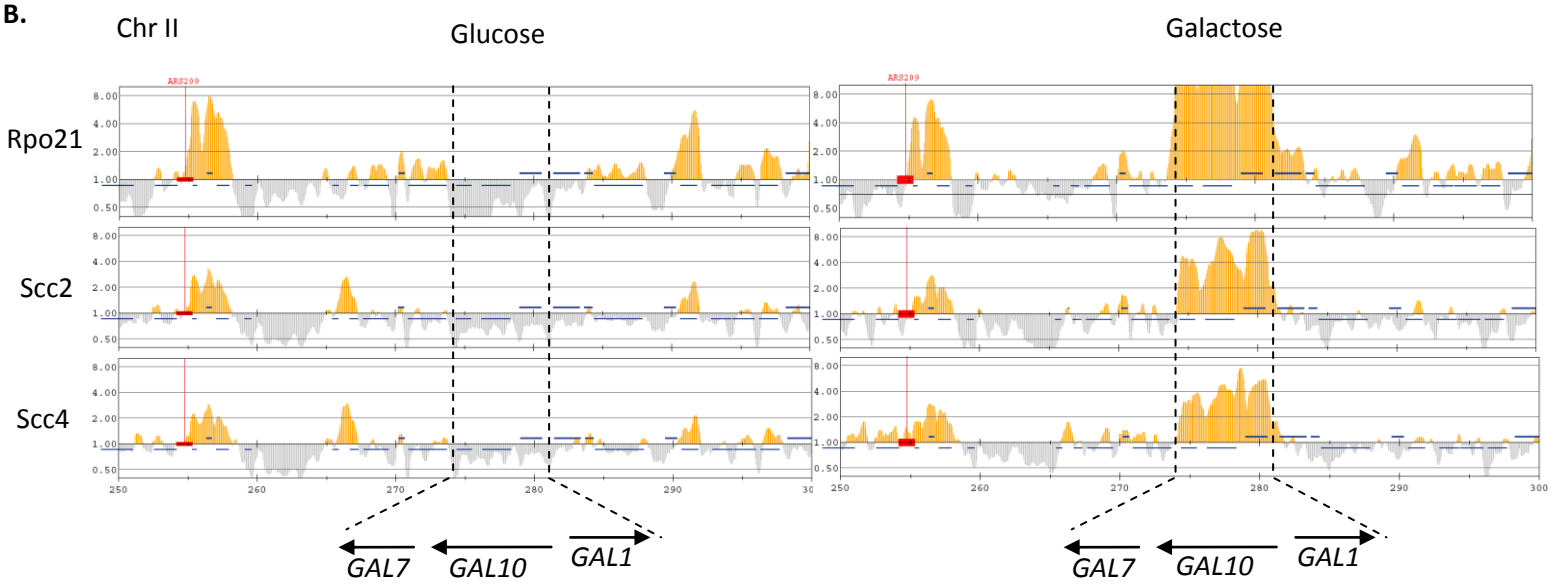

Figure S4. Correlation of Rpo21 with Scc2 at ORFs, related to Figure 4

(A) The ChIP-SEQ signals of Rpo21 and Scc2 at ORFs were used to calculate the correlation of Rpo21 with Scc2.

(B) Galactose-induced association of Rpo21 and Scc2/4 at a cluster of galactose-inducible genes. Exponentially-grown cells in glucose or galactose were used for ChIP-SEQ. Scc2/4 association was greatly increased at all 26 genes that associated with Pol II only in galactose and reduced at all 9 nine repressed by galactose. See also Figure 4.

Figure S5.

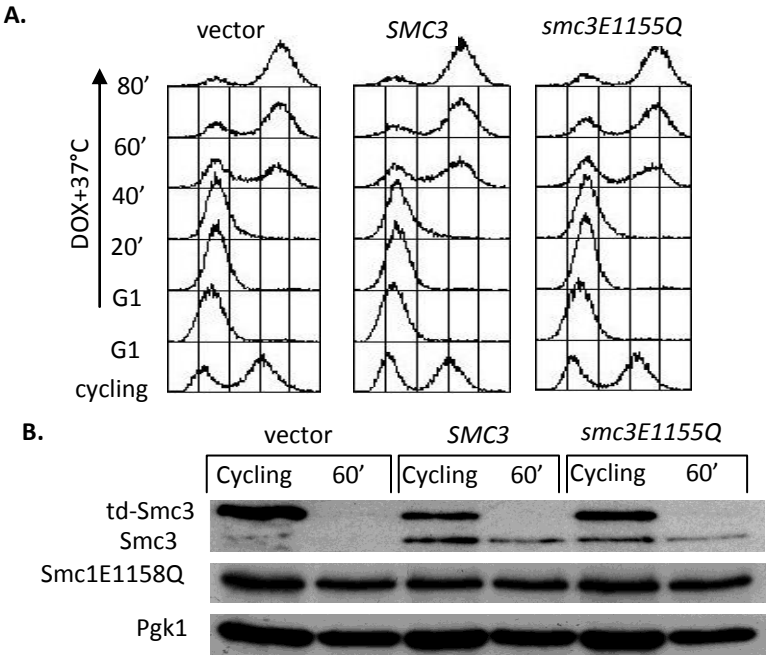

Figure S5. Cohesin completely blocked with NBDs stably engaged associates with centromeres

Cohesin incapable of hydrolysing ATP associated with both NBDs associates with centromeres. Exponential phase cells of strains K16331, K17240, K17241 and K17242 growing at 25°C were arrested in G1 with α-factor. Degradation of Smc3-td was induced and cells released from pheromone as in Figure 2E. (A) The DNA contents were measured by FACS. (B) The Smc3 proteins were detected by Weston blot.

Figure S6.

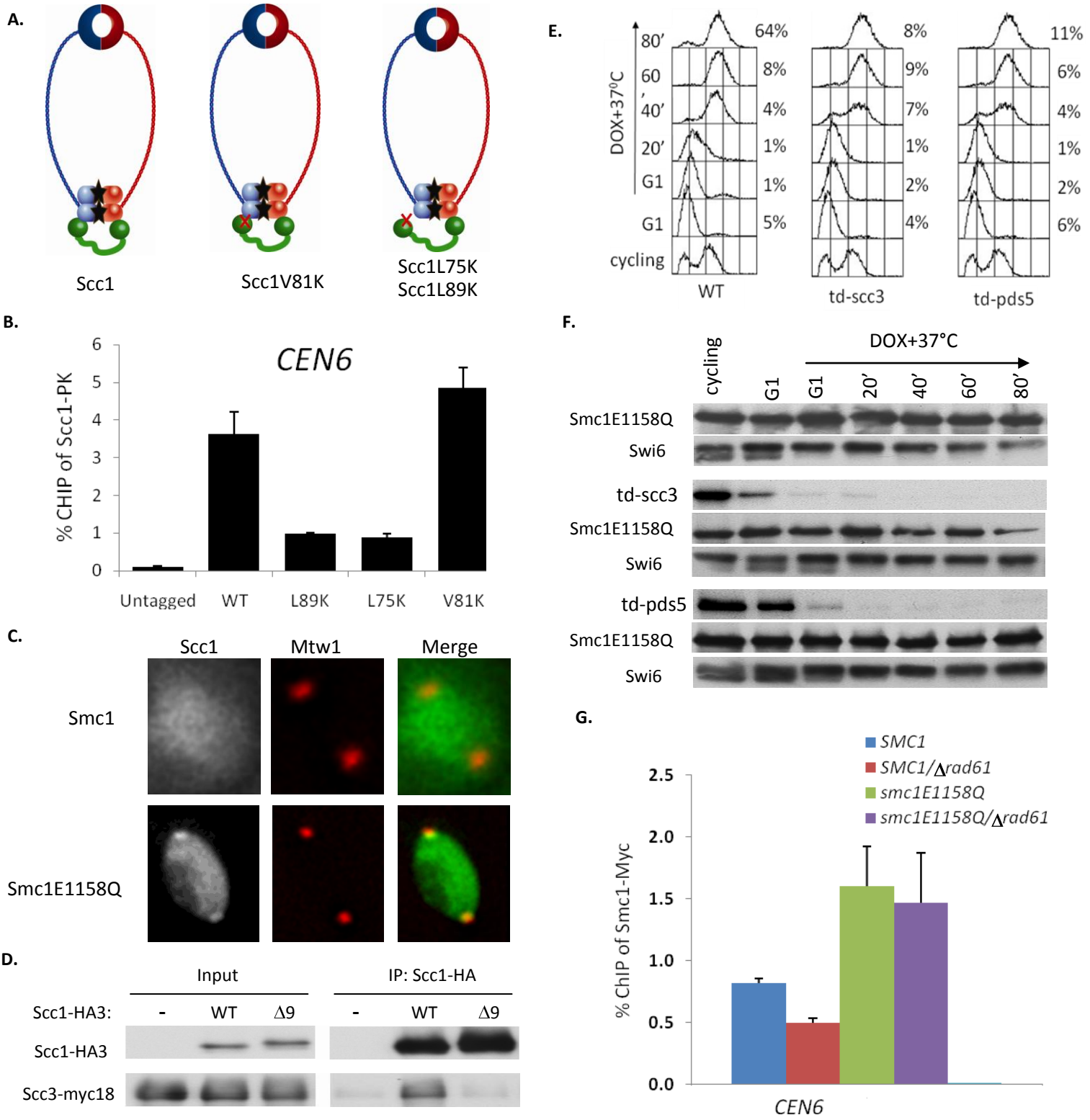

Figure S6. Ring formation and Scc3 are required for cohesin loading, related to Figure 6

(A) Mutations within Scc1's N-terminal domain that disrupt its interaction with Smc3's NBD.

(B) Ring formation is required for cohesin loading. ChIP-qPCR was performed for the quantitative measurement of chromatin association of PK9 tagged Scc1 WT and indicated mutants at Cen6. Mutations of L89K and L75K dramatically reduced Scc1 chromatin association. Error bars represent std. dev.; n=3.

(C) Localization of Scc1 with extra copy Smc1 or Smc1E1158Q during anaphase. Scc1-GFP co-expressed with extra copy Smc1 showed diffused localization in the nuclear, whereas Scc1-GFP co-expressed with Smc1E1158Q co-localized with Mtw1 during anaphase.

(D) Deletion of 9 amino acid residues (Δ319-327) within Scc1 disrupts it's interaction with Scc3. Yeast strains (K16634 and K16968) were grown to log phase in YPD medium. Cleared extracts were immunoprecipitated with anti-HA antibodies and Scc1-HA3 and Scc3-myc18 were detected with anti-HA and anti-myc antibodies, respectively. Scc1Δ319-327 (Δ9) cannot interact with Scc3.

(E) and (F) FACS analysis and Western bolt for Figure 6E.

(G) Association of myc9-tagged Smc1 or Smc1E1158Q with CEN6 measured by ChIP-qPCR in asynchronous YPD cultures of strains K699, K11850, K11857, K16780 and K16782. Error bars represent std. dev.; n=3.

Figure S7.

A.

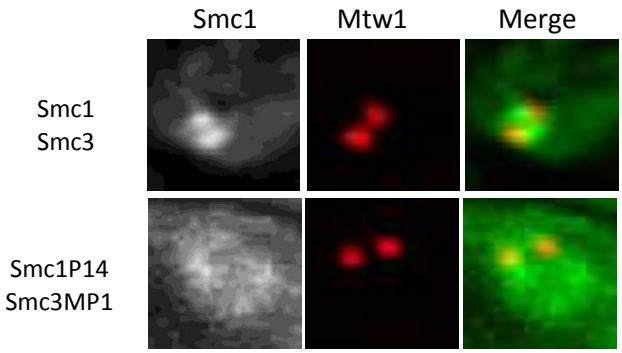

B.

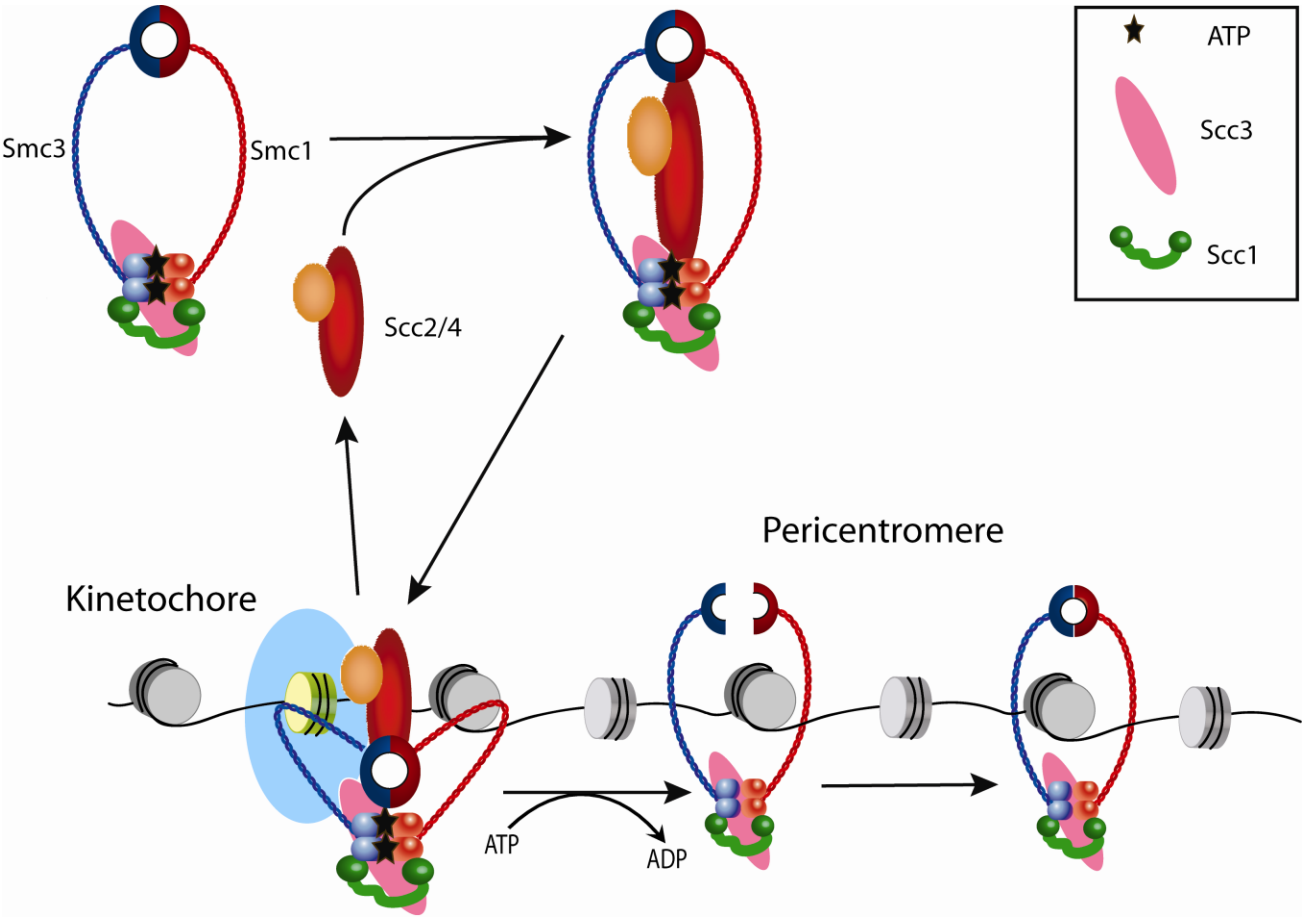

Figure S7. Smc1/3 hingles are required for cohesin loading, related to Figure 7

(A) Hinge-substituted SMC heterodimers cannot recruited to chromatin. Smc1-GFP or Smc1P14-GFP was co-expressed with extra copy of Smc3 or Smc3MP1 (K16946 and K16964). The GFP-fused proteins were visualized by fluorescence microscopy. As expected, Smc1-GFP formed a barrel structure. But the hinge-substitution of Smc1P14-GFP showed a diffused nuclear signal.

(B) Model for Scc2-dependent chromatin loading of cohesin. Following formation of tripartite rings and association with Scc3, ATP-driven NBD engagement and Scc2/4 promotes association with kinetochore proteins (blue) and interaction of closed Smc1/3 hinges with engaged NBDs. Hinges are opened by disengagement of NBDs driven by

ATP hydrolysis. Subsequent hinge re-association leads to chromatin entrapment, which then permits translocation from the initial entrapment site.

Supplemental Experimental Procedures

Chromatin Immunoprecipitation - Sequence assay:

Chromatin immunoprecipitation was carried out as previously described (Katou et al, 2003). DNA from WCE and ChIP fraction were further sheared to the average size of 150bp by ultra sonicator Covaris (Covaris, Inc.), end-repaired, ligated to sequencing adapters and amplified according to manufacturers instructions (Applied Biosystems SOLiD Library Preparation Protocol). Gel-purified amplified DNA between 100 and 150bp was sequenced on the Applied Biosystems Solid 3.5 platform to generate 50-bp reads. Sequence reads were aligned to the *S. cerevisiae* reference genome using Corona_lite (Applied Biosystems) allowing 3 color space mismatches. More than 10 million reads were successfully mapped for each sample (coverage is higher than 92% and redundancy is more than10 folds for each sample). Aligned reads were extended to 100 bp in the 3' direction. As inclusion of the repetitive data in ChIP-Seq experiments is critical for a complete understanding of protein localization along the chromosome (Rosenfeld *et al.*, 2009), sequence reads mapped to repetitive sequences were divided equally amongst all locations where the repetitive sequence appeared, treating each repetitive sequence as being equally responsible for the resulting sequencing read. The number of reads were summed up in a 500-bp window with a step size of 50-bp along the chromosome for ChIP and WCE fractions, respectively. After normalization of total reads of ChIP fraction against WCE fraction, enrichment values (ChIP/WCE) were calculated as previously described for each window and presented (Katou et al., 2003). All data were available from Gene Expression Omnibus (GEO) database with series number of **GSEXXXX**.

Purification of Smc1 and Smc3 head domains:

Smc3hd (M1-E190, 18 amino acid linker S1022-V1230) and Scc1-C (F451-A566) were fused to a 6xHis tag at the C-terminus in pET21 vectors. Smc1hd (M1-Q177, 31 amino acid linker, N1036-E1225) was cloned into a pET28 vector. Hydrolysis mutations (Smc1hdE1158Q, Smc3hdE1155Q) were introduced by site-directed mutagenesis PCR. Cells of the *E. coli* strain BL21(DE3)-RIPL were transformed with Smc3hd and co-transformed with Scc1-C and Smc1hd. Cultures were grown at 37°C until reaching an OD600 of 0.6, and expression was induced by addition of 1mM IPTG, for 12 hours at 20°C. Cells were harvested and resuspended in lysis buffer (50 mM Tris-HCl, pH 7.5, 250 mM NaCl, 1mM PMSF and complete protease inhibitor mix (Roche)) and lysed by French press (Constant System, UK) at 17 Kpsi. The supernatant was incubated with Talon Superflow beads (Clontech) for 2 hours at 4oC. Beads were washed with lysis buffer containing 10 mM imidazole (Sigma). Proteins were eluted in lysis buffer with 250mM imidazole and loaded onto a Superdex 200 16/60 size exclusion chromatography column (GE Healthcare) equilibrated with a buffer consisting of 100mM NaCl, 50mM Tris-HCl, pH 7.5, and 1mM β-ME. Peak fractions were collected and concentrated using Vivaspin columns (Sartorius Stedim biotech).

Analytical gelfiltration for binding analysis:

Superdex 200 10/300 GL gelfiltration columns (GE Healthcare) were used to investigate dimerisation between Smc1hd(1158Q)/Scc1-C and Smc3hd(1155Q). Before gel filtration, proteins were incubated at room temperature for 15 minutes. 100µl of 30µM Smc1hd/Scc1-C and Smc3hd were loaded together in the presence or absence of ATP at 0.5mM in a buffer consisting of 200mM NaCl, 50mM Tris-HCl, pH 7.5, 0.5mM $MgCl_2$. Fractions collected for each run were run on 11% SDS-PAGE and the proteins were visualized by Coomassie staining.

Depletion of degron fused proteins:

Exponentially grown yeast cells was arrested in G1 phase by adding 0.5 ng/ml α-factor and 0.5 µg/ml doxycycline at 25°C for 2.5 hours. To deplete degron fused proteins, cells were transferred into YPD medium containing 0.5 ng/ml of α-factor and 20 µg/ml of doxycycline at 37°C for 1 hour. Subsequently, cells were released from G1 arrest by being transferred in YPD medium containing 20 µg/ml of doxycycline and incubated at 37°C.

Co-immunoprecipitation assays:

Spheroplasts of yeast cells were prepared by zymolase and lysed in the lysis buffer (100mM KCl, 15mM $MgCl_2$, 0.025% Triton X100, 1mM DTT and 1mM PMSF). Protein concentration of the crude extract was measured by Bradford method. Five mg of the protein was incubated with anti-HA affinity matrix for 4 hours at 4^oC. After washing 5 times with lysis buffer the matrix was boiled in 2X Lamelli buffer. Samples were run on a 7.5% SDS-PAGE. For western analysis anti-HA, anti-Myc, and anti-Smc6 antibodies were used to probe for Smc3, Scc3 and Scc1 respectively.

Other techniques

Minichromosome cohesion assays were performed as described (Ivanov and Nasmyth, 2007). DNA content analysis (flow cytometry) were performed as described in Mishra *et al.*, 2010

Table S1. Summary of ChIP-SEQ

	Epitope tag	antibody			all mapped				uniquely mapped			
				All Tag	mapped Tag	mapped ratio(%)	covered region(%)	average redundancy	mapped Tag	mapped ratio(%)	covered region(%)	average redundancy
Smc3	HA3	BABCO, MMS-101P	IP	28,929,852	15,988,827	55.27	98.46	66.75	12,058,307	41.68	93.09	53.25
			WCE	27,155,235	15,883,057	58.49	98.19	66.50	12,124,888	44.65	92.75	53.74
Smc3E1155Q	HA3	BABCO, MMS-101P	IP	26,517,332	14,252,675	53.75	98.57	59.44	10,213,814	38.52	93.18	45.06
			WCE	25,494,590	14,649,054	57.46	98.27	61.28	11,728,829	46.01	92.87	51.92
Scc2	FLAG6	Sigma, F3165	IP	23,259,711	13,521,365	58.13	98.94	56.18	9,509,801	40.89	93.69	41.72
			WCE	31,573,873	17,153,868	54.33	98.78	71.39	13,544,778	42.90	93.55	59.52
Scc4	PK6	Serotec, MCA 1360	IP	24,758,698	13,381,314	54.05	98.92	55.61	9,997,636	40.38	93.67	43.88
			WCE	31,573,873	17,153,868	54.33	98.78	71.39	13,544,778	42.90	93.55	59.52
Rpo21	FLAG3	Sigma, F3165	IP	22,089,811	13,042,909	59.04	98.61	54.37	11,960,777	54.15	93.23	52.74
			WCE	31,573,873	17,153,868	54.33	98.78	71.39	13,544,778	42.90	93.55	59.52
Scc1(K16586)	PK9	Serotec, MCA 1360	IP	24,089,599	14,498,107	60.18	97.97	60.83	11,068,507	45.95	92.49	49.20
			WCE	27,342,256	15,758,470	57.63	98.88	65.51	13,186,020	48.23	93.46	58.00
Scc1(K16670)	PK9	Serotec, MCA 1360	IP	16,794,781	9,859,705	58.71	97.78	41.45	7,512,151	44.73	92.27	33.47
			WCE	24,242,112	12,746,042	52.58	98.49	53.20	7,780,383	32.09	93.06	38.80
Rpc128	FLAG6	Sigma, F3165	IP	9,070,646	4,569,270	50.37	91.33	20.57	3,071,951	33.87	85.65	14.74
			WCE	31,573,873	17,153,868	54.33	98.78	71.39	13,544,778	42.90	93.55	59.52
Spt15	FLAG6	Sigma, F3165	IP	8,200,526	4,410,241	53.78	94.88	19.11	2,994,441	36.52	89.27	13.79
			WCE	31,573,873	17,153,868	54.33	98.78	71.39	13,544,778	42.90	93.55	59.52

Table S2. List of Strains (all the strains were W303 background except indicated)

K699	*MATa, ade2-1, trp1-1, can1-100, leu2-3, 112, his3-11, 15, ura3, GAL, psi+*
K11850	*MATa, ura3::SMC1-Myc9::URA3*
K11852	*MATa, ura3::smc1K39I-Myc9::URA3*
K11854	*MATa, ura3::smc1S1130R-Myc9:: URA3*
K11857	*MATa, ura3::smc1E1158Q-Myc9:: URA3*
K11872	*MATa, leu2::smc3K38I-HA3::LEU2*
K11874	*MATa, leu2::smc3S1128R-HA3:: LEU2*
K13560	*MATa, leu2::SMC3-HA3::LEU2*
K13561	*MATa, leu2:: smc3E1155Q-HA3::LEU2*
K13585	*MATa, ura3::Smc3-MP1-hinge (259-263)-HA3 & Smc1-p14-hinge (250-251)::URA3*
K14133	*MATa, ura3::SMC1-Myc9::URA3, leu2::SMC3HA3::LEU2*
K14134	*MATa, ura3::smc1(F584R)-Myc9::URA3, leu2::SMC3HA3::LEU2*
K14601	*MATa, Scc1-PK9::KanMX,*
K14134	*MATa, Scc1-PK9::KanMX, scc2-4*
K16331	*MATa, bar1::hisG, UBR1::GAL1, 10p-Glu-UBR1/CMVp-tTA(HIS3), LEU2::pCM244*
K16335	*MATa, bar1::hisG, UBR1::GAL1, 10p-Glu-UBR1/CMVp-tTA(HIS3), leu2::pCM244, SMC1::kanMX-tetO2p-DHFRts-HA3-Smc1, ura3::SMC1-Myc9::URA3, TRP1-ARS1-CEN1(7.5kb minichromosome)*
K16336	*MATa, bar1::hisG, UBR1::GAL1, 10p-Glu-UBR1/CMVp-tTA(HIS3), LEU2::pCM244, SMC1::kanMX-tetO2p-DHFRts-HA3-Smc1, ura3::smc1K39I-Myc9::URA3, TRP1-ARS1-CEN1(7.5kb minichromosome)*
K16337	*MATa, bar1::hisG, UBR1::GAL1, 10p-Glu-UBR1/CMVp-tTA(HIS3), LEU2::pCM244, SMC1::kanMX-tetO2p-DHFRts-HA3-Smc1, ura3::smc1E1158Q-Myc9::URA3, TRP1-ARS1-CEN1(7.5kb minichromosome)*
K16338	*MATa, bar1::hisG, UBR1::GAL1, 10p-Glu-UBR1/CMVp-tTA(HIS3), LEU2::pCM244, SMC1::kanMX-tetO2p-DHFRts-HA3-Smc1, ura3::YIplac211, TRP1-ARS1-CEN1(7.5kb minichromosome)*
K16340	*MATa, bar1::hisG, UBR1::GAL1, 10p-Glu-UBR1/CMVp-tTA(HIS3), LEU2::pCM244, SMC3::kanMX-tetO2p-DHFRts-HA3-Smc3*
K16442	*MATa/α, Scc2-GFP::KanMX/Scc2-GFP::KanMX, Mtw1-RFP::KanMX/Mtw1-RFP::KanMX*
K16443	*MATa/α, Scc4-GFP::KanMX/Scc4-GFP::KanMX, Mtw1-RFP::KanMX/Mtw1-RFP::KanMX*
K16444	*MATa/α, ura3::SMC1-GFP::URA3/ura3::SMC1-GFP::URA3, Mtw1-RFP::KanMX/Mtw1-RFP::KanMX*
K16445	*MATa/α, ura3::smc1E1158Q-GFP::URA3/ura3::smc1E1158Q-GFP::URA3, Mtw1-RFP::KanMX/Mtw1-RFP::KanMX*
K16535	*MATa/α, ura3::3XtetO112::URA3, Scc2-PK1-TEV3-TETR::KANMX, Scc4-GFP::KANMX, Mtw1-RFP::KanMX/Mtw1-RFP::KanMX*
K16536	*MATa/α, ura3::SMC1-GFP::URA3/ura3::3XtetO112::URA3, Scc2-PK1-TEV3-TETR::KANMX,, Mtw1-RFP::KanMX/Mtw1-RFP::KanMX*
K16537	*MATa/α, ura3::smc1E1158Q-GFP::URA3/ura3::3XtetO112::URA3, Scc2-PK1-TEV3-TETR::KANMX,, Mtw1-RFP::KanMX/Mtw1-RFP::KanMX*
K16586	*MATa, Scc1-PK9::KanMX, R-CEN-R:CHRXIV, LEU2::pGal-recombinase;*
K16634	*MATa, SCC3-myc18::TRP1, leu2:: scc1(Δ319-327)-HA3::LEU2*
K16670	*MATa, Scc1-PK9::KanMX, LEU2::pGal-recombinase;* the endogenous cen14 was excised and cen14(332bp)-KlURA3 was integrated between ADE12 and ALG9
K16715	*MATa/α, leu2::smc3E1155Q-GFP::LEU2/leu2::smc3E1155QGFP::LEU2, Mtw1-RFP::KanMX/Mtw1-RFP::KanMX*
K16716	*MATa/α, leu2::smc3K38I-GFP::LEU2/leu2::smc3K38I-GFP::LEU2, Mtw1-RFP::KanMX/Mtw1-RFP::KanMX*
K16764	*MATa/α, trp1::SCC1-GFP::TRP1/trp1::SCC1-GFP::TRP1, ura3::Smc1E1158Q-Myc9::URA3/ura3::Smc1E1158Q-Myc9::URA3, Mtw1-RFP::KanMX/Mtw1-RFP::KanMX*
K16765	*MATa/α, trp1::scc1(V81K)-GFP::TRP1/trp1::scc1(V81K)-GFP::TRP1, ura3::Smc1E1158Q-Myc9::URA3/ura3::Smc1E1158Q-Myc9::URA3, Mtw1-RFP::KanMX/Mtw1-RFP::KanMX*
K16766	*MATa/α trp1::scc1(L75K)-GFP::TRP1/trp1::scc1(L75K)-GFP::TRP1, ura3::Smc1E1158Q-Myc9::URA3/ura3::Smc1E1158Q-Myc9::URA3, Mtw1-RFP::KanMX/Mtw1-RFP::KanMX*
K16767	*MATa/α, trp1::scc1(V89K)-GFP::TRP1/trp1::scc1(V89K)-GFP::TRP1, ura3::Smc1E1158Q-Myc9::URA3/ura3::Smc1E1158Q-Myc9::URA3, Mtw1-RFP::KanMX/Mtw1-RFP::KanMX*
K16780	*MATa, ura3::SMC1-Myc9::URA3, rad61::NatMX4*
K16782	*MATa, ura3::smc1E1158Q-Myc9::URA3, rad61::NatMX4*
K16795	*MATa/α, ura3::SMC1-GFP::URA3/ura3::SMC1-GFP::URA3, Mtw1-RFP::KanMX/Mtw1-RFP::KanMX, rad61::NatMX4/rad61::NatMX4*
K16796	*MATa/α, ura3::smc1E1158Q-GFP::URA3/ura3::smc1E1158Q-GFP::URA3, Mtw1-RFP::KanMX/Mtw1-RFP::KanMX, rad61::NatMX4/rad61::NatMX4*
K16799	*MATa, bar1::hisG, UBR1::GAL1, 10p-Glu-UBR1/CMVp-tTA(HIS3), LEU2::pCM244, SCC2::kanMX-tetO2p-DHFRts-HA3-SCC2, ura3::SMC1-Myc9::URA3*
K16800	*MATa, bar1::hisG, UBR1::GAL1, 10p-Glu-UBR1/CMVp-tTA(HIS3), LEU2::pCM244, SCC2::kanMX-tetO2p-DHFRts-HA3-SCC2, ura3::smc1E1158Q-Myc9::URA3*
K16811	*MATa, bar1::hisG, UBR1::GAL1, 10p-Glu-UBR1/CMVp-tTA(HIS3), LEU2::pCM244, ura3::SMC1-Myc9::URA3*
K16812	*MATa, bar1::hisG, UBR1::GAL1, 10p-Glu-UBR1/CMVp-tTA(HIS3), LEU2::pCM244, ura3::smc1E1158Q-Myc9::URA3*
K16874	*MATa, ura3::smc1E1158QP14-Myc9::URA3, leu2::Smc3MP1-HA3::LEU2*
K16895	*MATa/α, ura3::smc1(F584R/E1158Q)-GFP::URA3/ura3::Smc1(F584R/E1158Q)-GFP::URA3, leu2::SMC3-HA3::LEU2/leu2::SMC3-HA3::LEU2, Mtw1-RFP::KanMX/Mtw1-RFP::KanMX*
K16915	*MATa/α, trp1::scc1(Δ319-327)-GFP::TRP1/trp1::scc1(Δ319-327)-GFP::TRP1, ura3::Smc1E1158Q-Myc9::URA3/ura3::Smc1E1158Q-Myc9::URA3, Mtw1-RFP::KanMX/Mtw1-RFP::KanMX*
K16921	*MATa/α, ura3::smc1K39I-GFP::URA3/ura3::smc1K39I-GFP::URA3, Mtw1-RFP::KanMX/Mtw1-RFP::KanMX*
K16946	*MATa/α, ura3::SMC1-GFP::URA3/ura3::SMC1-GFP::URA3, leu2::SMC3-HA3::LEU2/ leu2::SMC3-HA3::LEU2, Mtw1-RFP::KanMX/Mtw1-RFP::KanMX*
K16963	*MATa/α, ura3:: smc1E1158QP14-GFP::URA3/ura3:: smc1E1158QP14-GFP::URA3, leu2::smc3MP1-HA3::LEU2/ leu2::smc3MP1-HA3::LEU2, Mtw1-RFP::KanMX/Mtw1-RFP::KanMX*
K16964	*MATa/α, ura3:: smc1P14-GFP::URA3/ura3:: smc1P14-GFP::URA3, leu2::smc3MP1-HA3::LEU2/ leu2::smc3MP1-HA3::LEU2, Mtw1-RFP::KanMX/Mtw1-RFP::KanMX*
K16968	*MAT α, SCC3-myc18::TRP1, leu2:: SCC1-HA3::LEU2*
K16982	*MATa/α, ura3::SMC1-GFP::URA3/ura3::SMC1-GFP::URA3, Mtw1-RFP::KanMX/Mtw1-RFP::KanMX, chl4::hph/chl4::hph*
K16983	*MATa/α, ura3:: smc1E1158Q-GFP::URA3/ura3:: smc1E1158Q-GFP, Mtw1-RFP::KanMX/Mtw1-RFP::KanMX, chl4::hph/chl4::hph*
K17000	*MATa, ura3::smc1(F584R/E1158Q)-Myc9::URA3, leu2::SMC3-HA3::LEU2*
K17026	*MATa/α, ura3:: smc1E1158Q-RFP::URA3/ura3:: smc1E1158Q-RFP, Scc2-GFP::KanMX/Scc2-GFP::KanMX, Mtw1-RFP::KanMX/Mtw1-RFP::KanMX*
K17027	*MATa/α, ura3:: smc1E1158Q-RFP::URA3/ura3:: smc1E1158Q-RFP Scc4-GFP::KanMX/Scc4-GFP::KanMX, Mtw1-RFP::KanMX/Mtw1-RFP::KanMX*
K17070	*MATa/α, ura3:: smc1E1158Q -GFP::URA3/ura3:: smc1E1158Q -GFP::URA3, leu2::SMC3-HA3::LEU2/ leu2:: SMC3-HA3::LEU2, Mtw1-RFP::KanMX/Mtw1-RFP::KanMX*
K17226	*MATa/α, Scc2-GFP::KanMX/Scc2-GFP::KanMX, Mtw1-RFP::KanMX/Mtw1-RFP::KanMX, chl4::hph/chl4::hph*

K17227	*MATa/α, Scc4-GFP::KanMX/Scc4-GFP::KanMX, Mtw1-RFP::KanMX/Mtw1-RFP::KanMX, chl4::hph/chl4::hph*
K17240	*MATa, bar1::hisG, UBR1::GAL1, 10p-Glu-UBR1/CMVp-tTA(HIS3), LEU2::pCM244, SMC3::kanMX-tetO2p-DHFRts-HA3-Smc3, ura3::smc1E1158Q-Myc9:: URA3, trp1::YIplac204*
K17241	*MATa, bar1::hisG, UBR1::GAL1, 10p-Glu-UBR1/CMVp-tTA(HIS3), LEU2::pCM244, SMC3::kanMX-tetO2p-DHFRts-HA3-Smc3, ura3::smc1E1158Q-Myc9:: URA3, trp1::SMC3-HA3::TRP1*
K17242	*MATa, bar1::hisG, UBR1::GAL1, 10p-Glu-UBR1/CMVp-tTA(HIS3), LEU2::pCM244, SMC3::kanMX-tetO2p-DHFRts-HA3-Smc3, ura3::smc1E1158Q-Myc9:: URA3, trp1::smc3E1155Q-HA3::TRP1*
K17299	*MATa, bar1::hisG, UBR1::GAL1, 10p-Glu-UBR1/CMVp-tTA(HIS3), LEU2::pCM244, SCC3::kanMX-tetO2p-DHFRts-HA3-SCC3, ura3::smc1E1158Q-Myc9::URA3*
K17300	*MATa, bar1::hisG, UBR1::GAL1, 10p-Glu-UBR1/CMVp-tTA(HIS3), LEU2::pCM244, PDS5::kanMX-tetO2p-DHFRts-HA3-PDS5, ura3::smc1E1158Q-Myc9::URA3*
K17458	*S288C, MATa, his3Δ1, leu2Δ0, met15Δ0, ura3Δ0, trp1Δ::hisG, SCC2-6His-6FLAG-loxP-KanMX-loxP*
K17459	*S288C, MATa, his3Δ1, leu2Δ0, met15Δ0, ura3Δ0, trp1Δ::hisG, SCC4-6PK::TRP1*
K17460	*S288C, MATa, his3Δ1, leu2Δ0, met15Δ0, ura3Δ0, trp1Δ::hisG, RPO21-6His-3FLAG-loxP-KanMX -loxP*
K18393	*S288C, MATa, his3Δ1, leu2Δ0, met15Δ0, ura3Δ0, trp1Δ::hisG, RPC128-6His-6FLAG-loxP-KanMX-loxP*
K18394	*S288C, MATa, his3Δ1, leu2Δ0, met15Δ0, ura3Δ0, trp1Δ::hisG, SPT15-6His-6FLAG-loxP-KanMX-loxP*

Table S3. List of ChIP-qPCR primers used for chromosome VI

Name	Position	Forward	Reverse
cen	DEG1	5’-GCGGCCTTAAGTTCGTAGTG-3’	5’- AAGTGCCGGAAATTGTCTTG-3’
Inner pericen	SPB4	5’-GACGAAAGAACGGAAACTCG-3’	5’- CCTTGGATAGCTTTGCTGGA-3’
Outer pericen	MSH4	5’-CCAGGATAGCCACTGCTTCT-3’	5’-CGATGACGTCGCTACACTT-3’
Inner arm	CMK1	5’-ACGGTTCAGTTCCTCCATTG-3’	5’- TGCAAAAGCTTTGCTGGTTA-3’
Outer arm	PAU5	5’-ACTCCGAGATTCTTGCTCCA-3’	5’-GCAGCAAATGTTGGGATTTA-3’
Lower cohesion	FAB1	5’-CCAGATGGCTCACAT-3’	5’-GCTCAGAATTGGGTTTGTC-3’

Supplemental Reference

Katou, Y., Kanoh, Y., Bando, M., Noguchi, H., Tanaka, H., Ashikari, T., Sugimoto, K., Shirahige, K. (2003) S-phase checkpoint proteins Tof1 and Mrc1 form a stable replication-pausing complex. Nature *424*:1078-1083.

Accession Numbers

All data were available from NCBI SRA (Sequence Read Archive) database with series number of SRP004703.